Mon. Not. R. Astron. Soc. **000**, 000–000 (0000) Printed 1 February 2008 (MN LaTeX style file v2.2)

On the potential of transit surveys in star clusters: Impact of correlated noise and radial velocity follow-up

Suzanne Aigrain[1,2] and Frédéric Pont[3]
[1] *Institute of Astronomy, University of Cambridge, Madingley Road, Cambridge, CB3 0HA, United Kingdom*
[2] *School of Physics, University of Exeter, Stocker Road, Exeter, EX4 4QL, United Kingdom*
[2] *Observatoire Astronomique de l'Université de Genève, 51, chemin des Maillettes, CH-1290 Sauverny, Switzerland*

Accepted ... Received ...; in original form...

ABSTRACT

We present an extension of the formalism recently proposed by Pepper & Gaudi to evaluate the yield of transit surveys in homogeneous stellar systems, incorporating the impact of correlated noise on transit time-scales on the detectability of transits, and simultaneously incorporating the magnitude limits imposed by the need for radial velocity follow-up of transit candidates. New expressions are derived for the different contributions to the noise budget on transit time-scales and the least-squares detection statistic for box-shaped transits, and their behaviour as a function of stellar mass is re-examined. Correlated noise that is constant with apparent stellar magnitude implies a steep decrease in detection probability at the *high* mass end which, when considered jointly with the radial velocity requirements, can severely limit the potential of otherwise promising surveys in star clusters. However, we find that small-aperture, wide field surveys may detect hot Neptunes whose radial velocity signal can be measured with present-day instrumentation in very nearby (< 100 pc) clusters.

Key words: planetary systems – surveys – techniques: photometric – open clusters and associations: general.

1 INTRODUCTION

Open Clusters have long been used as laboratories to test our understanding of star formation and stellar evolution, as each contains a (sometimes large) sample of stars with relatively well-known and common properties (age, composition, environment) but spanning a wide range of masses. For the same reasons, since the discovery of the first extra-solar planet around a Sun-like star in the field just over a decade ago (Mayor & Queloz 1995), the possibility of discovery extra-solar planets in open clusters has been a tantalising goal.

Open Clusters tend to be relatively distant, and their members relatively faint compared to the field stars usually targeted by radial velocity surveys. Most of the projects searching for extra-solar planets in Open Clusters therefore employ the transit technique, which is particularly well suited to dense stellar environments and has the additional advantage of providing a direct measurement of the planet to star radius ratio. Recent or ongoing transit surveys in Open Clusters include the UStAPS (the University of St Andrews Planet Search, Street et al. 2003; Bramich et al. 2005; Hood et al. 2005), EXPLORE-OC (von Braun et al. 2005), PISCES (Planets in Stellar Clusters Extensive Search, Mochejska et al. 2005, 2006), STEPSS (Survey for Transiting Extra-solar Planets in Stellar Systems, Burke et al. 2006) and the *Monitor* project (Aigrain et al. 2007).

Understanding the factors that affect the yield of such a survey is vital not only to maximise its detection rate, but also to enable the interpretation of the results of the survey, including in the case of non-detections, in terms of constraints on the incidence and parameter distributions of planetary companions. Recently, Pepper & Gaudi (2005a) (hereafter PG05a) introduced an analytical formalism to estimate the rate of detection of exo-planets via the transit method in stellar systems. One particularly interesting result is the fact that the probability that transits of a given system in a given cluster are detectable, if they occur, is a very slowly varying function of stellar mass in the regime where the photometric performance is dominated by the source photon noise, but drops sharply with stellar mass in the background-dominated regime. This implies

that the number of detections to be expected from a given survey is roughly proportional to the number of stars with source photon counts above the sky background level in that survey.

In a follow-up paper, Pepper & Gaudi (2005b) (hereafter PG05b) applied the aforementioned formalism to young open clusters, showing that transit surveys focusing on these systems have the potential to detect transiting Neptune and even Earth-sized planets, by making use of the fact that low-mass stars are relatively bright at early ages, and that their smaller radius gives rise to deeper transits for a given planet radius. This opens up the tantalising possibility of detecting transits of terrestrial planets from the ground, and what is more of doing so in young systems, where one might obtain particularly interesting constraints on the formation and evolution of extra-solar planets (Aigrain et al. 2007).

The formalism of PG05a assumes that the photometric errors on each star and in each observation are independent of each other (i.e. that the noise is white). However, an *a posteriori* analysis of the detection threshold of the OGLE transit survey in the light of their RV follow-up observations of OGLE candidate transits (Pont et al. 2005) demonstrated that the effective detection threshold is significantly higher than that expected for white noise only, suggesting that correlated noise on transit time-scales might be present in OGLE light curves. Pont, Zucker & Queloz (2006) (hereafter PZQ06) since developed a set of methods for evaluating the amount of correlated noise on transit time-scales in the light curves of transit surveys, and applied them to the OGLE light curves to show the latter do indeed contain correlated noise at the level of a few mmag. Similar analysis of light curves from other transit surveys (see e.g. Smith et al. 2006 and Irwin et al. 2007, and Pont 2007 for an overview) has since shown that they are also affected by correlated noise at a similar level. Because correlated noise does not average out as more observations of a given transit event are obtained, as white noise does, it is generally correlated noise which dominates over white noise in determining the detectability of transits around all but the faintest stars in a given field survey. A number of effects can give rise to correlated noise, including seeing-dependent contamination of the flux measured for a given star by flux from neighbouring stars, pointing drifts combined with flat-fielding errors, and imperfect sky subtraction – some or all of which may be important in a given survey depending on the telescope/instrument combination used and the observing strategy.

Photometry alone does not allow the mass of the companion causing the transits to be ascertained, and radial velocity measurements are thus generally needed to confirm the planetary nature of a transit event. As pointed out by PG05a, this effectively imposes an apparent magnitude limit for transit detections to be confirmable, as accurate radial velocity measurements of faint stars are extremely expensive in terms of large telescope time.

As noise that is correlated on transit timescales reduces the detectability of transits around the brightest stars in a given survey, but the need to perform radial velocity follow-up implies that only around the brightest stars can transits be confirmed, both effects must be incorporated in the scaling laws used to estimate the number of detections expected from a given survey. The present paper attempts to do this by extending the formalism of PG05a to include correlated noise and by translating the magnitude limit imposed by radial velocity follow-up into a cluster-specific mass limit.

Section 2 briefly sketches out the basics of the formalism of PG05a and describes how one or more additional noise terms representing correlated noise terms can be incorporated in it. The impact of these modifications on the noise budget on transit time-scales and on the transit detection probability as a function of mass are investigated in Section 3. Considerations external to the transit search itself, including radial velocity follow-up, are introduced in Section 4. Finally, the practical implications of the resulting formalism for Open Cluster transit searches are briefly explored in Section 5.

2 INTRODUCING RED NOISE TERMS

2.1 Overall formalism

This formalism is described in detail in PG05a, and only its major characteristics are sketched out here, so as to allow the modifications implied by the presence of correlated noise to be made clear.

PG05a compute the number of transiting planets with periods between P and $P+dP$ and radii between r and $r+dr$ that can be detected around stars with masses between M and $M+dM$ in a given stellar system as

$$\frac{d^3N_{\rm det}}{dM\ dr\ dP} = N_\star f_p \frac{d^2p}{dr\ dP}\mathcal{P}_{\rm tot}(M,\ P,\ r)\frac{dn}{dM}. \tag{1}$$

where $N_{\rm det}$ is the number of detected transiting planets, $N_\star$ is the total number of stars in the system, $d^2p/dr\ dP$ is the probability that a planet around a star in the system has a period between P and $P+dP$ and a radius between r and $r+dr$, f_p is the fraction of stars in the system with planets, $\mathcal{P}_{\rm tot}(M,\ P,\ r)$ is the probability that a planet of radius r and orbital period P will be detected around a star of mass M, and dn/dM is the mass function of the stars in the system, normalised over the mass range corresponding to $N_\star$.

Following Gaudi (2000), PG05a separate $\mathcal{P}_{\rm tot}(M,\ P,\ r)$ into three factors:

$$\mathcal{P}_{\rm tot}(M,\ P,\ r) = \mathcal{P}_{\rm tr}(M,\ P)\mathcal{P}_{\rm S/N}(M,\ P,\ r)\mathcal{P}_{\rm W}(P) \tag{2}$$

$\mathcal{P}_{\rm tr}$ is the probability that a planet transits its parent star, $\mathcal{P}_{\rm S/N}$ is the probability that, should a transit occur during a night of observing, it will yield a signal-to-noise ratio (S/N) that is higher than some threshold value, and $\mathcal{P}_{\rm W}$ is the window function that describes the probability that more than one transit will occur during the observations.

PG05a's expression for the transit probability is used without modification

$$P_{\rm tr} = \frac{R}{a} = \left(\frac{4\pi^2}{G}\right)^{1/3} M^{-1/3} R P^{-2/3} \tag{3}$$

where R is the star radius and a the orbital distance.

The S/N of a set of transits is $\mathrm{S/N} = \left(\Delta\chi^2_{\rm tr}\right)^{1/2}$, where $\Delta\chi^2_{\rm tr}$ is the difference in χ^2 between a constant flux and a boxcar transit fit to the data. PZQ06 give the general expression:

$$\Delta\chi^2_{\rm tr} = \frac{d^2}{\sigma_d^2} = \frac{d^2\, n^2}{\sum C_{ij}} \tag{4}$$

where d is the transit depth, σ_d is the uncertainty on the transit depth, n is the number of in-transit data points and C is the covariance matrix the in-transit flux measurements[1]. If the noise is uncorrelated, the non-diagonal elements of C are zero, and $\sum C_{ij} = \sum_i \sigma_i^2$ where σ_i is the uncertainty on the $i^{\rm th}$ flux measurement. Additionally, if this uncertainty is constant, i.e. $\sigma_i = \sigma_{\rm w}$, Equation (4) further reduces to:

$$\Delta\chi^2_{\rm tr} = n\left(\frac{\delta}{\sigma_{\rm w}}\right)^2, \tag{5}$$

which, for single transits, is equivalent to Equation (4) in PG05a. Note that the notation adopted here matches that of PZQ06, and thus differs that of PG05a,b. In particular, the symbols $N_{\rm tr}$ and n, used in PG05a,b to represent the number of in-transit points and the number of transits respectivtely, are inverted here. We also use σ_0 where PG05a,b used σ, and d where they used δ.

2.2 Modifying the detection statistic to account for red noise

In an attempt to account for the saturation of the rms. noise level that is seen at the bright end of all transit surveys, PG05a introduced in their Section 4.3 thqe concept of a *minimum observational error* $\sigma_{\rm sys}$, which is added in quadrature to the error contribution $\sigma_{\rm phot}$ from the sky and source photon noise to give the error estimate $\sigma_{\rm ind}$ for each data point:

$$\sigma_{\rm w} = (\sigma^2_{\rm phot} + \sigma^2_{\rm sys})^{\frac{1}{2}}. \tag{6}$$

This expression for $\sigma_{\rm w}$ is then simply inserted into Equation 5).

However, detailed analysis of the light curves of various transit surveys (PZQ06, Pont 2007) shows that they systematically contain noise that is correlated on transit timescales (2–3 h for a Hot Jupiter transit), i.e. the non-diagonal elements of the covariance matrix are non-zero. As a result, σ_d no longer decays as $n^{-1/2}$ as expected for uncorrelated (white) noise. PZQ06 propose a single parameter description of the covariance, assuming the noise can be separated into purely uncorrelated (white) and purely correlated (red) components, the former decaying as $n^{-1/2}$ but the latter independent of n:

$$\sigma_d^2 = \frac{\sigma_{\rm w}^2}{n} + \sigma_{\rm r}^2 \tag{7}$$

where $\sigma_{\rm w}$ and $\sigma_{\rm r}$ reresent the white and red noise components respectively. This single parameter description of the correlated noise assumes that the degree of correlation remains unchanged on all timescales up to the maximum transit duration. It is equivalent to approximating the covariance matrix with $C_{ii} = \sigma_0^2 \equiv \sigma_w^2 + \sigma_r^2$ in the diagonal, $C_{ij} = \sigma_r^2$ for two data points in the same transit, and $C_{ij} = 0$ otherwise (see Section for the treatment of multiple transits).

There is evidence that the correlation timescale in transit survey light curves is finite (Gould et al. 2006). If this correlation timescale is shorter than the maxium transit duration, the above expression would underestimate the significance of long-duration transit events. This does not appear to be the case for light curves analysed by PZQ06 and Pont (2007), where the noise remains correlated up to 3 h timescales. Nevertheless, it is interesting to investigate the impact of finite correlation timescales through a simple example. We consider a transit with a depth of 1% lasting 2 h and observed with 15 min time sampling, i.e. $n = 8$. In the white noise only case, if $\sigma_{\rm w} = 2$ mmag, $\sigma_d = 0.71$ mmag and $\Delta\chi^2_{\rm tr} = 200$. If correlated noise is present, with $\sigma_{\rm r} = 1$ mmag, the single parameter approximation gives $\sigma_d = 1.22$ mmag and $\Delta\chi^2_{\rm tr} = 67$. If on the other hand the noise is correlated only over timescales up to 1 h or 4 data points, i.e. $C_{ij} = 0$ for $|i-j| \geq 4$, $\sigma_d = 1.10$ mmag and $\Delta\chi^2_{\rm tr} = 82$. In general, even if the characteristic correlation timescale of the noise is shorter than a transit duration, we expect

[1] One can show that the estimate of d which minimises the χ^2 of the fit is the inverse-variance weighted average of the in-transit flux-measurements, and σ_d is thus the uncertainty on this average.

the single parameter correlated noise approximation adopted here to give an estimate of the transit significance that is much nearer to the true value than that obtained with the white noise approximation.

We therefore adopt Equation (7) for what follows. The white noise is assumed to be equal to the photon noise and modelled as of contributions from the source and the sky background:

$$\sigma_{\rm w}^2 = \sigma_{\rm source}^2 + \sigma_{\rm back}^2 = \frac{N_{\rm s} + N_{\rm b}}{N_{\rm s}^2}, \tag{8}$$

where $N_{\rm s}$ and $N_{\rm b}$ are the number of photons from the source and the sky detected in the photometric aperture.

PZQ06 found that the distribution of the rms. of OGLE light curves over a typical transit time-scale of 2.5 h is consistent with a constant red noise level of $\sigma_{\rm sys} \sim 3$ mmag, independent of apparent magnitude. Processing the light curves with a systematics removal algorithm such as Sys-Rem reduces $\sigma_{\rm sys}$ to ~ 1.5 mmag for the best objects. The work of the International Space Science Institute (ISSI) working group on transiting planets (Pont 2007) has shown that similar values are also typical of other surveys, with a correlated noise value of ~ 1.5 mmag for the best objects. We therefore adopt $\sigma_{\rm sys} \sim 1.5$ mmag throughout the following calculations, which would correspond to very good ground-based photometry. While it is theoretically possible to reduce the level of correlated systematics further, this value is used because it is considered representative of the leading surveys currently in operation.

In addition to this systematics term, a red noise component proportional to the white noise level (as a function of magnitude) is present in some surveys. This dominates over the systematics term in the domain where background photon noise dominates the white noise and is thus likely to be somehow associated with background subtraction. We therefore label it $\sigma_{\rm sub}$. For the purposes of the present calculations, it is modelled as a term proportional to the background noise:

$$\sigma_{\rm sub} = k\sigma_{\rm b} \tag{9}$$

For the purposes of the present work we assume $k = 0.2$. This is the kind of values the ISSI team found for the correlated noise in the HAT and SuperWASP surveys. Most cluster surveys, such as the University of St Andrews Planet Search (Street et al. 2003; Bramich et al. 2005; Hood et al. 2005), EXPLORE–OC (von Braun et al. 2005), STEPSS (Burke et al. 2006), PISCES (Mochejska et al. 2005; Hartman et al. 2005; Mochejska et al. 2006) or Monitor (Aigrain et al. 2007; Irwin et al. 2007), have 'better spatial sampling, and lower values of k might therefore be expected to apply, though preliminary analysis of test light curves indicates that $k \sim 0.2$ is also appropriate, if not an underestimate, for at least some of these surveys. In any case, this value is used here to illustrate the effects of noise of this type when it dominates the overall noise budget.

The overall red noise budget is thus

$$\sigma_{\rm r}^2 = \sigma_{\rm sys}^2 + \sigma_{\rm sub}^2 = \sigma_{\rm sys}^2 + \frac{k^2 N_{\rm b}}{N_{\rm s}^2}, \tag{10}$$

2.3 Multiple transits

As correlated noise does not average out over transit time-scales, but does average out over repeated transit events, it is particularly important to consider the repeatability of transits in the detection process when one suspects correlated noise might dominate. In an appendix, PG05a derived an expression for $\mathcal{P}_{\rm S/N}$ for multiple transits, which is based on the equation

$$\Delta_{\rm tr}^2(\text{multiple transits}) = N_{\rm tr}\ \Delta_{\rm tr}^2(\text{single transits}) = N_{\rm tr}\frac{d^2}{\sigma_d^2} \tag{11}$$

where $N_{\rm tr}$ is the number of observed transits. This equation remains valid in the presence of correlated noise provided there is no correlation over long timescales (similar to the planet's orbital period). In PG05a, $P_{\rm W}$ has to be calculated separately for each value of the number of transits. This assumes that the number of data points in each observed transit is the same, and in practice one must therefore choose a minimum value for the number of data points in a partially observed transit above which that transit contributes to $\mathcal{P}_{\rm W}$, and below which it does not.

PZQ06 provide a general formula which accounts for the number of data points in each observed transit:

$$\Delta_{\rm tr}^2(\text{multiple transits}) = n_{\rm tot}^2 \frac{d^2}{\sum_{k=1}^{N_{\rm tr}} n_k^2 \mathcal{V}(n_k)} \tag{12}$$

where $n_{\rm tot} = \sum_k = 1^{N_{\rm tr}}$ is the total number of in-transit points and

$$\mathcal{V}(n_k) \equiv \frac{1}{n_k^2} \sum^{n_k \times n_k \text{ block}} C_{ij} \tag{13}$$

is the noise integrated over the $k^{\rm th}$ observed transit. $\mathcal{P}_{\rm W}$ then becomes a multi-dimensional quantity dependent on not only $N_{\rm tr}$ but for each $N_{\rm tr}$, on the set of n_k. As with the PG05a formalism, it must be evaluated numerically.

In the present work, we make the assumption of homogeneous phase coverage, which allows us to ignore differences between n_k for the different transits, and enables us to (roughly) estimate the number of transits observed as a function of

period given the time sampling and survey duration. This can then be incorporated into Equation (11) directly, therefore alleviating the need to compute $P_{\rm W}$ separately. One can approximate $N_{\rm tr}$ as

$$N_{\rm tr} = \frac{t_{\rm tot}}{P} = \frac{N_{\rm n}\, t_{\rm night}}{P} \tag{14}$$

where $t_{\rm tot}$ is the total time spent on target, which is the product of the number of nights $N_{\rm n}$ and the average duration of a night $t_{\rm night}$, and P is orbital period. Reality diverges strongly from the homoegeneous phase coverage assumption close to harmonics of the daily interruptions in the observations, but it follows the global $1/P$ trend (see Fig. 1 of PG05a).

3 IMPACT ON THE NOISE BUDGET AND DETECTION STATISTIC

3.1 Noise budget on transit time-scales

Useful insights regarding the dominant noise sources, and how to mitigate those that have the largest impact on the transit detection performance, can be gained by exploring the dependency of the the various noise components on the stellar parameters. We start from the following expressions, given by PG05a, for $N_{\rm s}$, $N_{\rm b}$ and n (recalling that n is called $N_{\rm tr}$ in PG05a):

$$N_{\rm s} = \frac{L_{X,\odot} 10^{-0.4 A_X}}{4 \pi d^2} t_{\rm exp} \pi \left(\frac{D}{2}\right)^2 \left(\frac{M}{M_\odot}\right)^{\beta_X} = N_{\rm s,\odot} \left(\frac{M}{M_\odot}\right)^{\beta_X}, \tag{15}$$

$$N_{\rm b} = S_{{\rm sky},X} \Omega t_{\rm exp} \pi \left(\frac{D}{2}\right)^2, \tag{16}$$

and

$$n = \sqrt{1-b^2} \frac{R_\odot}{\delta t} \left(\frac{4P}{\pi G M_\odot}\right)^{1/3} \left(\frac{M}{M_\odot}\right)^{\alpha - \frac{1}{3}} = \sqrt{1-b^2}\; n_{\rm eq,\odot} \left(\frac{M}{M_\odot}\right)^{\alpha - \frac{1}{3}} \tag{17}$$

where M is the stellar mass; α is the index of the (power-law) mass-radius relation; β_X is the index of the (power-law) mass-luminosity relation in the filter X under consideration; D is the telescope aperture; $t_{\rm exp}$ is the exposure time; d is the distance to the cluster; A_X is the extinction to the cluster. PG05a adopt the distance-dependent extinction law $A_I = 0.5(d/{\rm kpc})$; $L_{X,\odot}$ is the Sun's photon luminosity in the filter of interest, which we compute, following PG05a, as

$$L_{X,\odot} = \frac{8 \pi^2 c R_\odot^2 \lambda_{X,c}^{-4} \Delta\lambda_X}{\exp\left(hc/\lambda_{X,c} k T_\odot\right) - 1}, \tag{18}$$

where $\lambda_{X,c}$ and $\Delta\lambda_X$ are the filter central wavelength and FWHM respectively; $S_{{\rm sky},X}$ is the sky photon flux per unit solid angle; Ω is the effective area of the seeing disk, which we compute, following PG05a, as

$$\Omega = \frac{\pi}{\ln 4} \theta_{\rm see}^2 \tag{19}$$

where $\theta_{\rm see}$ is the FWHM of the PSF; b is the impact parameter of the transit; δt is the interval between consecutive measurements. In PG05a,

$$\delta t = t_{\rm exp} + t_{\rm read} \tag{20}$$

where $t_{\rm read}$ is the readout time, which can be generalised to include any time spent off-target; $N_{\rm s,\odot}$ is the number of source photons in the aperture for a solar-mass star; $n_{\rm eq,\odot}$ is the number of points in an equatorial transit for a solar-mass star.

Substituting for $N_{\rm s}$ and $N_{\rm b}$ from Equations (15) and (16) into Equation (8) gives

$$\sigma_{\rm w}^2 = \frac{1}{N_{\rm s,\odot}} \left(\frac{M}{M_\odot}\right)^{-\beta_X} \left[1 + C_2 \left(\frac{M}{M_\odot}\right)^{-\beta_X}\right]. \tag{21}$$

where we have introduced, following PG05a,

$$C_2 = \frac{4 \pi d^2 S_{{\rm sky},X} \Omega}{L_{X,\odot} 10^{-0.4 A_X}} \tag{22}$$

which is the ratio of sky to source flux in the aperture for a solar mass star. Taking $\sigma_{\rm r}$ from Equation (10), $\sigma_{\rm w}$ from Equation (21) and n from Equation (17) and substituting into Equation (7),

$$\sigma_d^2 = \frac{\left(1-b^2\right)^{-1/2}}{N_{\rm s,\odot} n_{\rm eq,\odot}} \left(\frac{M}{M_\odot}\right)^{\frac{1}{3} - \alpha - \beta_X} \left[1 + C_2 \left(\frac{M}{M_\odot}\right)^{-\beta_X}\right] + \sigma_{\rm sys}^2 + \frac{k^2 C_2}{N_{\rm s,\odot}} \left(\frac{M}{M_\odot}\right)^{-2\beta_X}. \tag{23}$$

To simplify this expression we introduce two new constants

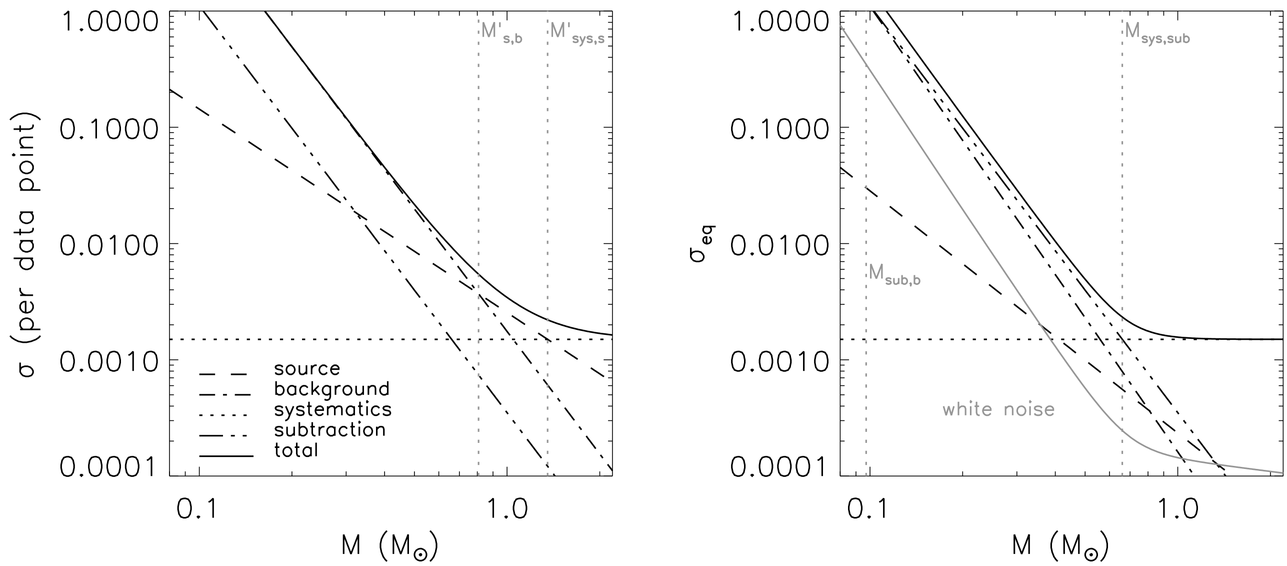

Figure 1. Error budget on individual data points (left) and over a the duration of an equatorial transit (right) for the fixed and fiducial parameters of PG05a, assuming $\sigma_{\rm sys} = 1.5\,$mmag and $k = 0.2$. The black dashed, dot-dash, triple dot-dash and dotted lines show the source photon noise, background photon noise, background subtraction noise and systematics terms respectively, and the solid black line shows the total noise budget. The grey line on the right panel shows what the behaviour the total noise would have it all the components behaved as white noise. The grey vertical dotted lines show mark transitions between the different regimes, as defined in Equations (27) to (30).

$$C_4 = N_{\rm s,\odot}\; n_{\rm eq,\odot} \tag{24}$$

which is the square of the background subtraction component for a Sun-like star, and

$$C_5 = \frac{k^2 C_2}{N_{\rm s,\odot}} \tag{25}$$

which is the total number of source photons collected during an equatorial transit for a Sun-like star. (Note that C_3 is defined in PG05a but not used here.) Equation (23) then becomes

$$\sigma_d^2 = \frac{\left(1-b^2\right)^{-1/2}}{C_4} \left(\frac{M}{M_\odot}\right)^{\frac{1}{3}-\alpha-\beta_X} \left[1 + C_2 \left(\frac{M}{M_\odot}\right)^{-\beta_X}\right] + \sigma_{\rm sys}^2 + C_5 \left(\frac{M}{M_\odot}\right)^{-2\beta_X}. \tag{26}$$

The form of $\sigma_{\rm eq}$, the depth uncertainty for equatorial transits ($b = 0$) and of the different terms that compose it is illustrated in Figure 1 (right panel). Also shown for comparison is the noise level *per data point* (left panel), or $\mathcal{V}(1)$.

The relative importance of the red noise components is clearly enhanced over the transit time-scale. While the systematics term is the same for all stellar masses, the source photon noise is a steeply decreasing function of stellar mass, the background subtraction noise is even steeper, and the background photon noise is the steepest. There may thus be up to four noise regimes, starting with the systematics-limited regime at the highest masses, followed by the source noise-limited regime, the subtraction-limited regime, and finally the background noise-limited regime at the lowest masses.

Equating each pair of components and solving for M yields the mass regimes in which each component dominates. This exercise was done by PG05a to obtain $M_{\rm sky}$, the transition mass between the source and background noise-limited regimes, which for clarity we rename $M_{\rm s,b}$.

$$M_{\rm s,b} = C_2^{\frac{1}{\beta_X}}\, M_\odot \tag{27}$$

Given the two additional noise terms that have been introduced, the relevant transitions are now:

$$M_{\rm sys,s} = \left(C_4\; \sigma_{\rm sys}^2\right)^{\frac{3}{1-3\alpha-3\beta_X}}\; M_\odot \tag{28}$$

$$M_{\rm s,sub} = \left(C_4\; C_5\right)^{\frac{3}{1-3\alpha+3\beta_X}}\; M_\odot \tag{29}$$

$$M_{\rm sub,b} = \left(\frac{C_4\; C_5}{C_2}\right)^{\frac{3}{1-3\alpha}}\; M_\odot \tag{30}$$

However, it is very easy for the source noise-limited regime to disappear altogether, because the source photon noise averages out over the duration of the transit whereas the systematics and background subtraction noise do not. Even if one ignores the background subtraction term, the source-limited regime disappears if $M_{\rm s,b} \geq M_{\rm sys,s}$. Given the set of fixed and fiducial parameters adopted by PG05a, the source limited regime exists only if $\sigma_{\rm sys} < 0.5$ mmag. Adopting a more realistic value of 1.5 mmag, there is a direct transition between the systematics- and subtraction-limited regime, which occurs at

$$M_{\rm sys,sub} = \left(\frac{C_5}{\sigma_{\rm sys}^2}\right)^{\frac{1}{2\beta_X}} M_\odot. \tag{31}$$

For the subtraction-dominated regime to exist requires k to be relatively large ($k \geq 0.2$). If this is not the case, there is a direct transition between the systematics and background limited regimes:

$$M_{\rm sys,b} = \left(\frac{C_4\,\sigma_{\rm sys}^2}{C_2}\right)^{\frac{3}{1-3\alpha-2\beta_X}} M_\odot. \tag{32}$$

3.2 Detection probability $\mathcal{P}_{\rm S/N}$

The detection probability is derived following the same method as PG05a, although we consider multiple, rather than single transits.

A transit observed $N_{\rm tr}$ times is assumed to be detectable if it gives rise to a detection statistic $\Delta\chi^2_{\rm tr} \geq \Delta\chi^2_{\rm min}$. If equatorial transits of a given system are detectable, one can derive a maximum impact parameter $b_{\rm max}$ up to which transits of such a system are also discoverable (PG05a). This arises because $n = t_{\rm eq}\sqrt{1-b^2}/\delta t$, where b is the impact parameter of the transit and $t_{\rm eq}$ the duration of an equatorial transit:

$$t_{\rm eq} = R\left(\frac{4P}{\pi G M}\right)^{\frac{1}{3}} \tag{33}$$

where R is the radius and M the mass of the star. We have assumed that the planet radius $r \ll R$ and ignored limb-darkening, which allows us to ignore grazing transits as both extremely rare and hard to detect, and to write $\delta = (r/R)^2$ where r is the planet radius.

Therefore, the probability that transits of such a system are detectable, i.e. that $\Delta\chi^2_{\rm tr} \geq \Delta\chi^2_{\rm min}$, reduces to $\mathcal{P}_{\rm S/N} = b_{\rm max}$ when integrated over b, assuming the impact parameters are uniformly distributed between 0 and 1. However, the statement:

$$\Delta\chi^2_{\rm tr} = \Delta\chi_{\rm eq}\sqrt{1-b^2}, \tag{34}$$

which is valid in PG05a, no longer holds here, because $\Delta\chi^2_{\rm tr}$ is no longer simply proportional to n. Instead, Equations (4) and (7) imply:

$$\Delta\chi^2_{\rm tr} = N_{\rm tr}\;\delta^2\left(\frac{\sigma_{\rm w}^2}{n} + \sigma_{\rm r}^2\right)^{-1} = N_{\rm tr}\;\delta^2\left(\frac{\sigma_{\rm w}^2}{n_{\rm eq}\sqrt{1-b^2}} + \sigma_{\rm r}^2\right)^{-1}. \tag{35}$$

The expression for $b_{\rm max}$ is found by setting the left hand side of Equation (35) to $\Delta\chi^2_{\rm min}$ and solving for b. This yields:

$$\mathcal{P}_{\rm S/N} = b_{\rm max} = \sqrt{1 - \left[\frac{\sigma_{\rm w}^2}{n_{\rm eq}}\left(\frac{N_{\rm tr}\;\delta^2}{\Delta\chi^2_{\rm min}} - \sigma_{\rm r}^2\right)^{-1}\right]^2} \tag{36}$$

Inserting the expressions for the different noise terms derived above gives:

$$\mathcal{P}_{\rm S/N} = \sqrt{1 - \left\{\frac{\left(\frac{M}{M_\odot}\right)^{\frac{1}{3}-\alpha-\beta_X}\left[1 + C_2\left(\frac{M}{M_\odot}\right)^{-\beta_X}\right]}{C_4\left[\frac{N_{\rm tr}}{\Delta\chi^2_{\rm min}}\left(\frac{r}{R_\odot}\right)^4\left(\frac{M}{M_\odot}\right)^{-4\alpha} - \sigma_{\rm sys}^2 - C_5\left(\frac{M}{M_\odot}\right)^{-2\beta_X}\right]^{-1}}\right\}^2}. \tag{37}$$

This expression reduces, in the case of white noise only – i.e. when $\sigma_{\rm sys}$ and k vanish – to PG05a's Equation (15). A similar expression for $\Delta\chi^2_{\rm eq}$, the detection statistic for equatorial transits, also ensues:

$$\Delta\chi^2_{\rm eq} = \frac{N_{\rm tr}\left(\frac{r}{R_\odot}\right)^4\left(\frac{M}{M_\odot}\right)^{-4\alpha}}{C_4\left(\frac{M}{M_\odot}\right)^{\frac{1}{3}-\alpha-\beta_X}\left[1 + C_2\left(\frac{M}{M_\odot}\right)^{-\beta_X}\right] + \sigma_{\rm sys}^2 + C_5\left(\frac{M}{M_\odot}\right)^{-2\beta_X}}. \tag{38}$$

If $\Delta\chi^2_{\rm eq} < \Delta\chi^2_{\rm min}$ for a particular star-planet system, transits of that systems are not detectable, whatever the inclination.

[t]

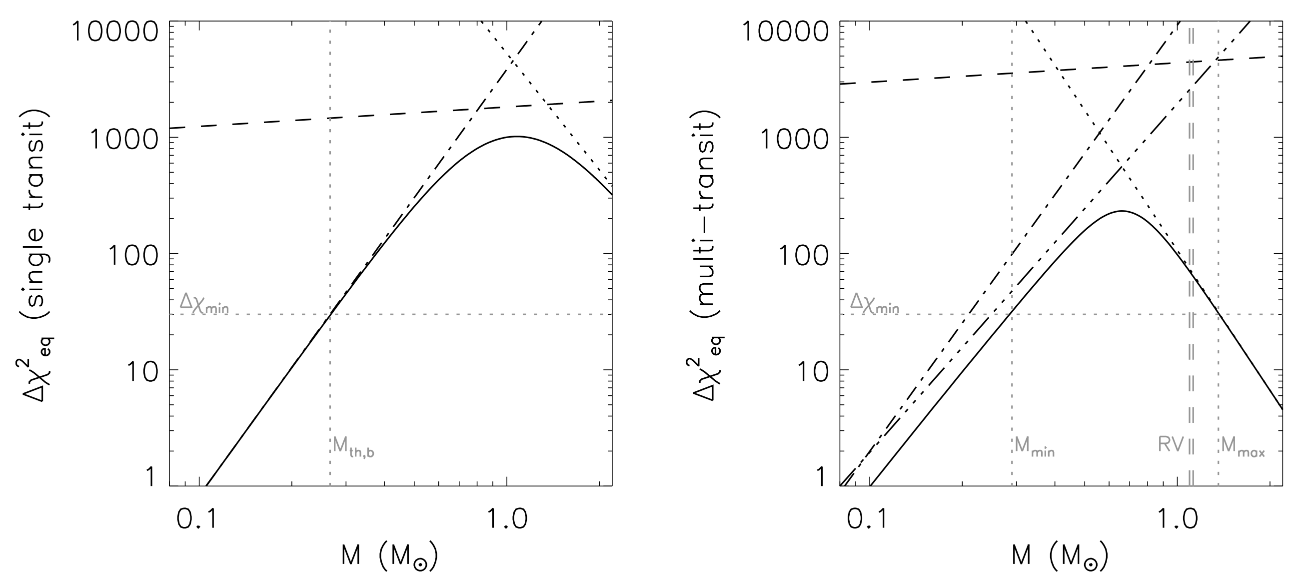

Figure 2. Detection statistic $\Delta\chi^2_{\rm eq}$ for an equatorial transit, for individual transits and assuming the systematics are white (as in PG05a, left) or for multiple transits and incorporating both red noise terms with $\sigma_{\rm sys} = 1.5$ mmag and $k = 0.2$ (this work, right). The line styles have the same meaning as in Figure 1. The grey horizontal dotted line marks the detection threshold $\Delta\chi^2_{\rm min} = 30$ adopted by PG05a. The grey vertical dotted lines mark the lower and, if applicable, upper mass limits between which the transits are detectable. The grey vertical dashed lines mark the mass range where RV follow-up is feasible with FLAMES+UVES.

The overall behaviour of $\Delta\chi^2_{\rm eq}$ as a function of mass is illustrated in Figure 2 (right panel). Also shown for comparison is the single-transit $\Delta\chi^2_{\rm eq}$ obtained following PG05a, i.e. assuming the systematics are white (left panel).

PG05a point out that, using $\alpha = 1$ and $\beta_I = 3.5$, $\Delta\chi^2_{\rm eq} \propto M^{1/6}$ and $M^{11/3}$ in the source and background noise-limited regimes respectively, which has the remarkable implication that the detectability of planetary transits is virtually independent of mass for all stars above sky, while it decreases rapidly for stars below sky. In white, source limited noise only, the number of detections from a given survey is thus roughly proportional to the number of unsaturated stars above sky. In the red noise-limited regimes, $\Delta\chi^2_{\rm tr}$ no longer depends on n, i.e. on b (provided the transit is not grazing, a given transit event contributes the same amount to the detectability no matter what the number of observations in that transit). Transits of a given system are thus detectable, whatever the inclination (i.e. the transit duration), if they are deep enough (δ) and enough of them are observed ($N_{\rm tr}$). Using the same values of α and β_I as in PG05a, $\Delta\chi^2_{\rm eq} \propto M^{-4}$ and M^3 in the systematics and background-limited regimes respectively, with the remarkable implication that transits are detectable only around stars *below* a certain mass, determined by the systematics term. The reason is that the degree of correlation of the noise lowers the advantage of having longer transits and lower photon noise (a larger and brighter primary) compared to that of having deeper transits (a smaller primary).

The combined effect of the different noise terms across the entire stellar mass range is to give rise to a peak in $\Delta\chi^2_{\rm eq}$ versus M, as illustrated by Figure 2. This immediately points to a potentially very simple way of evaluating wether a given type of planet is detectable at all in a given cluster with a given observational setup: find the 'peak mass', or stellar mass at which $\Delta\chi^2_{\rm eq}$ is maximised, by differentiating Equation (38) with respect to M and setting the derivative to zero:

$$C_4 \left(\frac{M}{M_\odot}\right)^{\frac{1}{3}-\alpha-\beta_X} \left[5\alpha + \beta_X - \frac{1}{3} + C_2 \left(5\alpha + 2\beta_X - \frac{1}{3}\right) \left(\frac{M}{M_\odot}\right)^{-\beta_X}\right] + C_5 \left(1 + 2\beta_X\right) \left(\frac{M}{M_\odot}\right)^{-2\beta_X} + \sigma^2_{\rm sys} = 0. \quad (39)$$

The solution of Equation (39) could then be plugged back into Equation (38), to yield $\Delta\chi^2_{\rm peak}$. If $\Delta\chi^2_{\rm peak} > \Delta\chi^2_{\rm min}$, detections are possible in the cluster under consideration. In that case, one can also compute the limits $M_{\rm low}$ and $M_{\rm up}$ of the stellar mass range over which detections are possible by setting the left hand side of Equation (38) to $\Delta\chi^2_{\rm min}$ and solving for M. In practice, both equations cannot be solved analytically in the general case. If one is interested in calculating precise values of $\Delta\chi^2_{\rm peak}$, $M_{\rm low}$ and $M_{\rm p}$, the simplest way is to to compute $\Delta\chi^2_{\rm eq}$ for a range of M and find the quantities of interest numerically.

However, as discussed in Section 3.1, it is not uncommon for a single component to dominate over a significant portion of the mass regime. By considering dependence of $\Delta\chi^2_{\rm eq}$ on each of the components one at a time, one can obtain useful insights

into what limits the transit survey's performance, and what mass range will be accessible. Each of the source, background and background subtraction terms imply a minimum mass around which a given type of transit is detectable:

$$M_{\rm low,s} = \left(C_1'\right)^{\frac{3}{-9\alpha+3\beta_X-1}} M_\odot \tag{40}$$

$$M_{\rm low,b} = \left(C_1'\ C_2\right)^{\frac{3}{-9\alpha+6\beta_X-1}} M_\odot \tag{41}$$

$$M_{\rm low,sub} = \left(C_1'\ C_4\ C_5\right)^{\frac{1}{4\alpha-2\beta_X}} M_\odot \tag{42}$$

where C_1' is a multiple-transit equivalent of PG05a's C_1:

$$C_1' = \frac{C_1}{N_{\rm tr}} = \frac{\Delta\chi^2_{\rm min}}{N_{\rm tr}\ N_{\rm s,\odot}\ n_{\rm eq,\odot}} \left(\frac{r}{R_\odot}\right)^{-4} \tag{43}$$

and $M_{\rm low,s}$ and $M_{\rm low,b}$ are equivalent to PG05a's $M_{\rm th,s}$ and $M_{\rm th,b}$. On the other hand, the systematics term implies a maximum mass:

$$M_{\rm up} = \left(\frac{1}{C_1'\ C_4\ \sigma^2_{\rm sys}}\right)^{\frac{1}{4\alpha}} M_\odot \tag{44}$$

Note that PG05a's white systematic noise term also induces an upper mass limit detection, but it is typically larger than $3\,M_\odot$. As long as $M_{\rm up}$ is above the peak of the mass function, correlated systematic noise will not significantly affect the total number of detections in a given survey. However, it does have the effect of preventing detections around the brightest stars, which are arguably the most interesting, because of their enhanced potential for follow-up.

In general, more than one component contributes near the limits of the range of masses of stars around which transits of a given type of planet are detectable, and the expressions for $M_{\rm low}$ and $M_{\rm up}$ are rather complex. Again, an alternative is to compute each term in $\Delta\chi^2_{\rm eq}$ for an array of stellar masses and to find the values of M between which $\Delta\chi^2_{\rm eq} > \Delta\chi^2_{\rm min}$.

4 ADDITIONAL CONSIDERATIONS

4.1 Turnoff mass

Following PG05a, we compute the turnoff mass

$$M_{\rm to} = \left(\frac{\epsilon M_\odot^\beta c^2}{L_{\rm bol,\odot} A}\right)^{1/(\beta-1)} \tag{45}$$

where ϵ is the efficiency of Hydrogen burning and β is the bolometric mass-luminosity index.

4.2 Saturation mass

Also following PG05a's expression for the number of photons at the peak of the PSF of a given star, the saturation mass is

$$\left(\frac{M_{\rm sat}}{M_\odot}\right)^{\beta_X} = \frac{4\pi d^2}{L_{X,\odot}}\ 10^{0.4A_X}\ \left[\left(\frac{D}{2}\right)^{-2} \frac{N_{\rm FW}}{t_{\rm exp}\pi} - S_{{\rm sky},X}\theta^2_{\rm pix}\right] \left\{1 - \exp\left[-\ln 2\left(\frac{\theta_{\rm pix}}{\theta_{\rm see}}\right)^2\right]\right\}^{-1} \tag{46}$$

where $N_{\rm FW}$ is the full-well capacity of the detector and $\theta_{\rm pix}$ is the angular size of the pixels.

4.3 Radial velocity follow up

Radial velocity (RV) follow-up is necessary to confirm the planetary nature of any detected transits and to measure companion masses. In this section,we examine the range of stellar masses over which this is feassible for a planet of a given mass and period.

PG05a used a fixed magnitude limit ($V = 17$ or $V = 18$) beyond which planets were considered undetectable by the radial velocity method. This is approximately suitable for planetary companions to Sun-like stars: it is extremely difficult to measure radial velocities with precisions of a few tens of m/s level beyond $V \sim 18$ even with the largest telescopes available at present (Pont et al. 2005). However, in cluster transit searches, many of the detections occur around lower-mass stars, where planetary companions may induce significantly larger radial velocity modulations, and a more detailed treatment is needed.

For a star of a given magnitude, the minimum detectable radial velocity amplitude $K_{\rm min}$ is highly instrument dependent, and we examine two representative telescope / instrument combination: the UV-Visual Echelle Spectrograph (UVES) coupled to the Fibre Large Area Multi-Element Spectrograph (FLAMES) on the Very Large Telescope (VLT) – hereafter FLAMES+UVES – and the High Accuracy Radial velocity Planet Searcher on the 3.6 m telescope at La Silla – hereafter

HARPS. High precision measurements tend to be limited by instrument stability rather than by photon noise, in the sense that, if deemed interesting enough, a given (short-period) object can be observed as long as necessary, binning the phase-folded measurements to reduce the photon noise contribution. However, for each telescope / instrument combination there is also a magnitude limit $Y_{\rm RV}$, beyond which the signal-to-noise ratio achievable in a single exposure drops below a critical level, and high precision measurements are no-longer feasible in reasonable exposure times. As the spectral region used typically covers the V and R-bands, Y should be either V or R, depending on which filter the object under consideration is brightest in.

The radial velocity semi-amplitude induced by a given planet scales as

$$K \propto m P^{-1/3} M^{-2/3} \tag{47}$$

where m is the planet mass and we have assumed that $m \ll M$ and that the inclination of the system is edge-on. All planets giving rise to $K \geq K_{\rm min}$ are then assumed to be detectable around stars with apparent magnitude down to $Y_{\rm RV}$, beyond which it is assumed that high precision radial velocity measurements are not feasible at all with the telescopes/instruments under consideration. For HARPS, we use $Y = V$ and $Y_{\rm RV} = 14$, for FLAMES+UVES we use $Y = R$ and $Y_{\rm RV} = 18$. Both are relatively optimistic limits. This means that in each cluster, there is a lower mass limit

$$M_{\rm RV,min} = 10^{M_{Y,\odot} - Y_{\rm RV} + 5 \log d - 5 + A_Y / 2.5 \beta_Y} \tag{48}$$

where Y is R or V, below which no radial velocity measurements are feasible with a given instrument, and above which the minimum detectable planet mass is

$$m_{\rm min} = m_{\rm ref} \left(\frac{P}{3 \text{ days}} \right)^{1/3} \left(\frac{M}{M_\odot} \right)^{2/3} \tag{49}$$

where $m_{\rm ref} = M_{\rm Neptune}$ for HARPS and $M_{\rm Jupiter}$ for FLAMES+UVES. If considering a particular planet mass m across a range of stellar masses, one can derive a maximum stellar mass $M_{\rm RV,max}$ around which such a planet produces a detectable RV signal by setting $M_{\rm min}$ in Equation (49) to m:

$$M_{\rm RV,max} = \left(\frac{m}{m_{\rm ref}} \right)^{3/2} \left(\frac{P}{3 \text{ days}} \right)^{-1/2} M_\odot \tag{50}$$

which is independent of the cluster properties and depends on the planet mass and period only. Planets with mass m and period P can thus be confirmed by radial velocity with present observational means only if they orbit stars with $M_{\rm RV,min} < M < M_{\rm RV,max}$.

Note that, for the sake of simplicity, we have ignored a number of important factors, including morphological differences in the spectra of stars of different types and the impact of rotation, which broadens the lines and degrades the radial velocity precision.

5 APPLICATIONS

One can roughly evaluate the mass range $[M_{\rm min}; M_{\rm max}]$ within which planets of a given radius and period in a given cluster produce detectable transits *and* RV modulations:

$$M_{\rm min} = \max \left(M_{\rm low}, M_{\rm RV,min} \right) \tag{51}$$

$$M_{\rm max} = \min \left(M_{\rm up}, M_{\rm to}, M_{\rm sat}, M_{\rm RV,max} \right) \tag{52}$$

5.1 PG05a's fiducial cluster

Going back to the fiducial cluster of PG05a, under the relatively optimistic assumption that $\sigma_{\rm sys} = 1.5$ mmag, the detection of transits alone for a 1 $M_{\rm Jupiter}$ planet in a 2.5-d orbit is possible around stars with masses between 0.28 and 1.49 $M_\odot$. However, using FLAMES+UVES on the VLT, for which we assume that $K_{\rm min}$ corresponds to a Jupiter mass planet in the same orbit around the same star and that $R_{\rm RV} = 18$, $M_{\rm RV,min} = 1.13\, M_\odot$ and $M_{\rm RV,max} = 1.22\, M_\odot$, so that the mass range where such a planet can be detect via transits *and* radial velocity is only 0.11 $M_\odot$.

The combination of correlated systematics and follow-up requirements imposes very stringent limits on the potential of transit surveys in open clusters. In practice, it implies an even stronger dependence on cluster distance that illustrated in the bottom right panel of PG05a's Figure 8.

5.2 Example galactic open clusters

In a subsequent paper, PG05b applied the formalism of PG05a to a number of well-studied Galactic open clusters and, on this basis, made the prediction that close-in Neptune- or even Earth-sized planets should be detectable in some of these clusters

Name	Distance (pc)	Age (Myr)	Aperture (m)	$t_{\rm exp}$ (s)	$M_{\rm low}$ ($M_\odot$)	(Cause)	$M_{\rm up}$ ($M_\odot$)	(Cause)	ΔM ($M_\odot$)
Hyades	46	625	1.8	15	0.15	(lim)	0.55	(sat)	0.47
Praesepe	175	800	1.8	45	0.15	(lim)	0.87	(sat)	0.79
NGC 2682 (M67)	783	4000	3.6	45	0.15	(lim)	1.36	(TO)	1.28
NGC 2168 (M35)	912	180	3.6	45	0.15	(lim)	1.49	(sys)	1.41
NGC 2323 (M50)	1000	130	3.6	45	0.15	(lim)	1.49	(sys)	1.41
NGC 2099 (M37)	1513	580	3.6	45	0.15	(lim)	1.49	(sys)	1.41
NGC 6819	2500	2900	6.5	45	0.15	(lim)	1.49	(sys)	1.41
NGC 1245	2850	960	6.5	45	0.15	(lim)	1.49	(sys)	1.39
NGC 6791	4800	8000	6.5	45	0.15	(lim)	1.08	(TO)	0.92

Table 1. Masses ranges over which transits of Jupiter-sized planets in 2 d orbits are detectable in selected Galactic open clusters, using the observational parameters of PG05b. Columns 7 and 9 give the primary cause of the upper and lower limits (sat: saturation; TO: turn-off; sys: systematics; lim: lower limit of mass range considered).

Name	Aperture (m)	$t_{\rm exp}$ (s)	$M_{\rm low}$ ($M_\odot$)	(Cause)	$M_{\rm up}$ ($M_\odot$)	(Cause)	ΔM ($M_\odot$)
Hyades	0.1	30	0.15	(lim)	0.79	(sat)	0.70
Praesepe	0.1	30	0.18	(RV)	1.22	(RV)	1.04
NGC 2682 (M67)	0.8	15	0.57	(RV)	1.22	(RV)	0.66
NGC 2168 (M35)	1.3	15	0.64	(RV)	1.22	(RV)	0.59
NGC 2323 (M50)	1.5	15	0.66	(RV)	1.22	(RV)	0.57
NGC 2099 (M37)	2.7	15	0.75	(RV)	1.22	(RV)	0.48
NGC 6819	5.0	15	0.84	(RV)	1.22	(RV)	0.38
NGC 1245	6.5	18	0.93	(RV)	1.22	(RV)	0.30
NGC 6791	6.5	65	1.07	(RV)	1.08	(TO)	0.01

Table 2. Masses ranges over which transits and radial velocity modulations of Jupiter-sized planets in 2 d orbits are detectable in selected Galactic open clusters, using SuperWASP for the Hyades and Praesepe and the observational parameters of PG05b for the other clusters, and using FLAMES+UVES for radial velocity follow-up. Columns 7 and 9 give the primary cause of the upper and lower limits (RV: radial velocity).

via transit surveys from ground-based 2- to 6-m class telescopes. If so, transit surveys in open clusters might not only enable the detection of planets around well characterised stars of known age and metallicity, but may also lead to the first radius measurements for terrestrial planets. It is therefore interesting to investigate the detectability of Jupiter-sized and smaller planets in these clusters in the presence of red noise.

We use the same test sample of 9 clusters (the Hyades, Praesepe, M67, M35, M50, M37, NGC 6819, NGC 1245 and NGC 6791) as PG05b, from which we take the cluster parameters (distance, age, extinction) and the observational parameters, which are similar to those of PG05a except that the night duration is $t_{\rm night} = 8$ h, the telescope apertures are 1.8 m (Pan-STARRS), 3.6 m (CFHT) and 6.5 m (MMT) depending on the cluster (as selected by PG05b), and the exposure time is $t_{\rm exp} = 45$ s for all clusters except the Hyades for which $t_{\rm exp} = 15$ s.

Table 1 shows the range of stellar masses between which transits Jupiter-sized planets in 2 d orbits produce detectable transits. For all but the most distant cluster, transits are detectable right down to the minimum stellar mass considered ($0.15\,M_{\rm odot}$, well below the limit of $0.3\,M_\odot$ adopted by PG5b), i.e. the addition of a correlated background subtraction term component does not affect the results. For all but the nearest clusters, the upper limit comes from the systematics term ($M_{\rm up} = 1.49\,M_{\rm sun}$, independent of the cluster and observational parameters). For the Hyades and Praesepe, the upper limit is saturation with the observational setup considered here, but this can be raised by using shorter exposure times and / or smaller telescopes, which have the added advantage of providing wider fields of view. For example, the SuperWASP project Pollacco et al. (2006) uses multiple 11 cm apertures and has 13.5 as pixels and an effective bandpass similar to R ($S_{\rm sky}\sim$). As it cycles between fields, $\delta = 8$ min. With the standard exposure times of 30 s, we obtain $M_{\rm sat} = 0.79\,M_\odot$ for the Hyades and $1.71\,M_\odot$ for Praesepe. These represent a significant gain, and hereafter we adopt these observational parameters for these two clusters. Note that one could decrease the exposure time for the Hyades to increase $M_{\rm sat}$ further, but this would conflict with the primary goal of SuperWASP, namely to search for transits around field stars. Overall, correlated noise does not strongly affect the detectability of transits of hot Jupiters in these clusters.

We now incorporate the limits induced by radial velocity follow-up with FLAMES+UVES in the calculations. The results are shown in Table 2. Radial velocity or turnoff are now the limiting factors in almost all cases, and imply a stronger distance

Name	Aperture (m)	$t_{\rm exp}$ (s)	$M_{\rm low}^{(1)}$ ($M_{\odot}$)	(Cause)	$M_{\rm low}^{(2)}$ ($M_{\odot}$)	(Cause)	$M_{\rm up}$ ($M_{\odot}$)	(Cause)	ΔM ($M_{\odot}$)
Hyades	0.1	30	0.08	(lim)	0.28	(RV)	0.50	(sys)	0.42
Praesepe	1.8	15	0.08	(lim)	0.63	(RV)	0.52	(sys)	0.44
NGC 2682 (M67)	1.8	15	0.18	(back)	1.06	(RV)	0.52	(sys)	0.34
NGC 2168 (M35)	3.6	15	0.16	(back)	1.19	(RV)	0.52	(sys)	0.36
NGC 2323 (M50)	3.6	15	0.18	(back)	1.25	(RV)	0.52	(sys)	0.34
NGC 2099 (M37)	3.6	15	0.32	(back)	1.49	(RV)	0.49	(sys)	0.17
NGC 6819	6.5	15	0.39	(back)	1.70	(RV)	0.46	(sys)	0.07

Table 3. Masses ranges over which transits of Neptune-sized planets in 2 d orbits are detectable (1) and confirmable with HARPS (2) in selected Galactic open clusters, using SuperWASP for the Hyades and the observational parameters of PG05b for the other clusters.

dependence of the planet yield than transits. It is interesting to note, however, that confirmed detections of transiting hot Jupiters are possible down to very low stellar masses in the nearest clusters.

We also investigate the detectability of Neptune-sized planets, using HARPS for radial velocity follow-up, still with a period of 2 d. For such planets, the systematics term implies an upper mass limit of $M_{\rm up} = 0.53\,M_{\odot}$ independent of the observational set-up. We use the same observational setup as before except for Praesepe, where a greater photon-collecting capacity than SuperWASP's is needed to offset the smaller planet radius, so we revert to Pan-STARRS. The results are shown in Table 3. We have omitted NGC 1245 and NGC 6791 because transits of Neptune-sized planets are not detectable at all in these clusters. The systematics term severely limits the maximum stellar mass around which transits of hot Neptunes can be detected, while the need for radial velocity measurements limits the minimum mass around which they can be confirmed, and it is only in the Hyades that confirmed transiting Neptunes are expected to be detectable. We stress that these limits are relatively independent of theobservational setup.

For hot Earths, the systematics term implies a very stringent upper limit of $M_{\rm up} = 0.13\,M_{\odot}$, and the formalism adopted here also precludes radial velocity confirmation around any stars in the clusters condidered (although it may be feasible to detect the radial velocity signal from a hot Earth around a bright star using HARPS by observing many repetitions of the orbit).

6 CONCLUSIONS

Simple modifications have been made to the formalism of PG05a to account for correlated noise and the need for RV follow-up. These should lead to more realistic estimates of the efficiency of Open Cluster transit surveys, while retaining the analytic nature of the original formalism, which affords useful insights into the behaviour of the detection probability as a function of mass.

Two types of correlated noise were considered: systematics, which are constant with apparent stellar magnitude, and background subtraction noise, which scales with the background photon noise level. The latter behaves in a similar fashion to background photon noise itself, though its contribution to the total noise budget on transit time-scales has a slightly less steep dependence on the stellar mass, and therefore it does not significantly modify the yield of a survey unless extreme assumptions are adopted. However, the former implies a detection probability that steeply decreases with increasing mass and therefore curtails detections at the bright end. This effect is much stronger than the loss of sensitivity implied by a white minimum observational error of similar magnitude.

In the course of evaluating the impact of correlated noise on the detectability of transits, we made a number of simplifying assumptions, and these should be borne in mind when comparing the predictions of the present formalism to the yield of real cluster transit surveys. First, we have assumed that the noise budget is the same for all stars of a given magnitude, and that every data point in a given light curve is affected by the same noise level. In fact, both white and correlated noise typically affect some objects and/or nights more than others, as they depend on factors which vary from object to object (e.g. crowding, position on the detector, colour) and time (e.g. weather, instrumental problems). Additionally, the way we compute the number of observed transits does not take into account the very strong features close to integer multiples of a day that are present in the window function of most ground-based surveys. As a result, while the scaling laws derived here apply for the majority of the objects in a given survey, the most significant detections in a real survey may well occur in special cases where the time sampling and the noise characteristics were particularly favourable.

On the other hand, the radial velocity modulation induced by the companion in the primary, in order to measure the companion's mass, is only detectable given present day instrumentation over a certain stellar mass range which can be close to, if not above, the maximum mass implied by the systematics term for typical targets and observational set-ups. Thus, even though correlated systematics may not affect the yield of Open Cluster transit surveys significantly in terms of transit

detection alone (because transits usually remain detectable around stars close to the peak of the mass function), it has a very serious impact on the yield in terms of transits whose planetary nature can be confirmed and where the companion mass can be measured. While the specific colour-magnitude relation followed by the members of a given cluster may enable one to exclude many of the astrophysical false positives which affect all transit surveys without actually detecting the radial velocity modulation of the primary, the scientific impact of any detection of a transiting planet will be significantly lowered if its mass cannot be measured.

To illustrate a possible application of this modified formalism, it was applied to a selection of well-studied Galactic Open Clusters, which were used by PG05b to show that transits of Hot Neptunes, and even Hot Earths, should be detectable from the ground in nearby young Open Clusters. While correlated noise alone has little effect on the detectability of hot Jupiters in these clusters, we find that radial velocity follow-up severely limits the minimum mass around which their masses can be measured, which makes the confirmation of even Jupiter-mass planets in the more distant clusters difficult. Additionally, correlated systematics at the level of 1.5 mmag affecting all stars in a 20 night survey imply that transits of hot Neptunes are only detectable around stars with masses below $0.5\,M_{\odot}$. For such low stellar masses, the planetary radial velocity signal will only be measurable in very nearby clusters ($< 100\,pc$) with present-day facilities. If hot Neptunes are abundant around M-stars, some could be detected by the combination of small aperture, wide field surveys such as SuperWASP and state of the art radial velocity instruments such as HARPS.

The same level of systematics limits the detection of transits of Hot Earths to stars with masses below $0.13\,M_{\odot}$, irrespective of the cluster properties or observational setup. It is thus vital to achieve lower systematics (e.g. by going to space with CoRoT and Kepler) to detect transits of terrestrial planets, and particularly to detect them around stars bright enough that it may be possible to measure their radial velocity signal with future instrumentation.

A general trend that emerges from this work is that the combination of correlated noise and RV follow-up requirements severely limits the choice of suitable target clusters, and effectively imposes a rather stringent distance limit. Additionally, we note that, for a given cluster, the optimal observational setup differs depending on the type of planet considered.

ACKNOWLEDGEMENTS

This work was initiated in the course of the meetings of the International Team on Transiting Planets set up in 2005 under the auspices of the International Space Science Institute (ISSI), and we are indebted to all the members of this team for invigorating discussions and useful feedback. SA gratefully acknowledges support from a PPARC Postdoctoral Research Fellowship. This work has been done in the context of the preparation to the CoRoT data analysis, for which FP acknowledges support from a PRODEX grant. The authors are also grateful to the referee, Scott Gaudi, for his careful reading of the manuscript and his useful comments and suggestions.

REFERENCES

Aigrain S., Hodgkin S., Irwin J., Hebb L., Irwin M., Favata F., Moraux E., Pont F., 2007, MNRAS, in press

Bramich D. M., Horne K., Bond I. A., Street R. A., Cameron A. C., Hood B., Cooke J., James D., Lister T. A., Mitchell D., Pearson K., Penny A., Quirrenbach A., Safizadeh N., Tsapras Y., 2005, MNRAS, 359, 1096

Burke C. J., Gaudi B. S., DePoy D. L., Pogge R. W., 2006, AJ, 132, 210

Gaudi B. S., 2000, ApJL, 539, L59

Gould A., Dorsher S., Gaudi B. S., Udalski A., 2006, AcA, 56, 1

Hartman J. D., Stanek K. Z., Gaudi B. S., Holman M. J., McLeod B. A., 2005, AJ, 130, 2241

Hood B., Cameron A. C., Kane S. R., Bramich D. M., Horne K., Street R. A., Bond I. A., Penny A. J., Tsapras Y., Quirrenbach A., Safizadeh N., Mitchell D., Cooke J., 2005, MNRAS, 360, 791

Irwin J., Irwin M., Aigrain S., Hodgkin S., Hebb L., Moraux E., 2007, A&A, in press

Mayor M., Queloz D., 1995, Nature, 378, 355

Mochejska B. J., Stanek K. Z., Sasselov D. D., Szentgyorgyi A. H., Adams E., Cooper R. L., Foster J. B., Hartman J. D., Hickox R. C., Lai K., Westover M., Winn J. N., 2006, AJ, 131, 1090

Mochejska B. J., Stanek K. Z., Sasselov D. D., Szentgyorgyi A. H., Bakos G. Á., Hradecky J., Devor V., Marrone D. P., Winn J. N., Zaldarriaga M., 2005, AJ, 129, 2856

Pepper J., Gaudi B. S., 2005a, ApJ, 631, 581

Pepper J., Gaudi B. S., 2005b, Acta Astronomica, 56, 183

Pollacco D. L., Skillen I., Cameron A. C., Christian D. J., Hellier C., Irwin J., Lister T. A., Street R. A., West R. G., Anderson D., Clarkson W. I., Deeg H., Enoch B., Evans A., Fitzsimmons A., Haswell C. A., Hodgkin S., Horne K., Kane S. R. e. a., 2006, PASP, 118, 1407

Pont F., 2007, in Afonso C., Weldrake D., Henning T., eds, Transiting Extrasolar Planets ASP Conf. Ser., Detection capacities of ground-based transit surveys (the ISSI team on exoplanet transits)
Pont F., Bouchy F., Melo C., Santos N. C., Mayor M., Queloz D., Udry S., 2005, A&A, 438, 1123
Pont F., Zucker S., Queloz D., 2006, MNRAS, 373, 231
Smith A. M. S., Collier Cameron A., Christian D., Clarkson W. I., Enoch B., Evans A., Haswel C., Hellier C., Horne K., J. I., Kane S. R., Lister T. A., Norton J., et al. 2006, MNRAS, 373, 1151
Street R. A., Horne K., Lister T. A., Penny A. J., Tsapras Y., Quirrenbach A., Safizadeh N., Mitchell D., Cooke J., Cameron A. C., 2003, MNRAS, 340, 1287
von Braun K., Lee B. L., Seager S., Yee H. K. C., Mallén-Ornelas G., Gladders M. D., 2005, PASP, 117, 141